



Structure of Si/Ge nanoclusters: Kinetics and thermodynamics

Ari Harjunmaa^{a,*}, Kai Nordlund^a, Alexander Stukowski^b

^a Department of Physics, University of Helsinki, P.O. Box 43, FIN-00014 Helsinki, Finland

^b Institut für Materialwissenschaft, Technische Universität Darmstadt, Darmstadt, Germany

ARTICLE INFO

Article history:

Received 1 October 2010

Received in revised form 2 November 2010

Accepted 7 December 2010

Available online 31 December 2010

Keywords:

Molecular dynamics

Cluster

Si

Ge

ABSTRACT

The optimal structure and element distribution of $\text{Si}_x\text{Ge}_{1-x}$ clusters was investigated in terms of free energy. The methods employed were computational simulations based on classical molecular dynamics. Clusters obtained in our previous work were further simulated through annealing at different temperatures. In addition, a combination of molecular dynamics and a semi-grand-canonical Monte Carlo algorithm was used to find a free-energetically favorable element configuration for the clusters. The results show that annealing at conventional temperatures improves the clusters' sphericity only slightly, and they remain much more amorphous than clusters cut out from crystalline bulk; only at extreme annealing temperatures are the sphericity and crystallinity notably improved. Furthermore, Ge atoms are found to segregate to the surface of the clusters, which greatly reduces the free energy of the clusters.

© 2010 Elsevier B.V. All rights reserved.

1. Introduction

Ionized cluster beam deposition is a bottom-up method capable of producing a variety of nanomaterials, many of which cannot be produced by any other method [1–3]. Varying the deposition parameters results in an array of different possibilities for the structure of the produced films [4–6]. The particular characteristics of these materials are made possible by quantum effects [7], resulting mainly from the conservation of the original morphology of the deposited clusters.

Attention has turned in particular to silicon clusters due to the discovery of their strong visible photoluminescence at room temperature, a trait not shared by bulk silicon [7,8]. The photoluminescence of nanocrystalline germanium and Si/Ge has also been investigated to reveal a similar effect [9,10]. This characteristic of semiconductor clusters persists even when deposited *en masse* – again, as long as the morphology of the original clusters remains intact, such as in porous films [6].

The experimental work done on this subject has been complemented by a multitude of numerical simulations (e.g. [11,12]). In these simulations, clusters are usually prepared as perfect spheres cut out from a bulk crystal and relaxed using thermal annealing. This, however, is not a realistic way of recreating real clusters, since in experimental applications, clusters are made using bottom-up methods. For instance, in gas-condensation-type sources, the cluster material is sputtered from a magnetron, and the atoms are swept into a condensation chamber by a flow of inert gas (e.g.

argon), which cools the vapor, allowing it to condensate into clusters [13].

We have previously simulated the formation of silicon, germanium, and Si/Ge clusters in an argon atmosphere to recreate the above process using molecular dynamics (MD) [14]. The results showed that while there was a tendency towards the formation of spherical clusters, not all clusters were able to reach a radially symmetrical form in the time frame of MD simulations. Whether this was an effect of short simulation time (of the order of nanoseconds), or if the resulting shapes were indeed stable, was left as an open issue. In addition, it was noted that germanium atoms displayed the tendency to segregate to the outer atomic layers of the clusters, which confirmed earlier findings done in our group [15].

This work continues the investigation of the energetically favorable shape and element distribution of Si and Ge clusters. In addition to the traditional MD method, which we now use to anneal the least spherical of the clusters to prompt radial symmetry, we also use a new method that combines MD with a semi-grand-canonical Monte Carlo (SGCMC) algorithm to investigate the element distribution that is most favorable in terms of the free energy of the clusters.

2. Method

The basis of the simulations done for this work is classical molecular dynamics [16]. Two different MD simulation programs were used: for pure MD simulations, the program PARCAS [17]; and for the mixed MD/SGCMC simulations, the program LAMMPS [18]. For both programs, the atomic interactions were realized

* Corresponding author. Tel.: +358 919150617.

E-mail address: ari.harjunmaa@helsinki.fi (A. Harjunmaa).

using the Tersoff potential for Si and Ge [19]. In all simulation runs, the temperature was controlled using the Berendsen temperature control algorithm [20] with a time constant of 250 fs.

The PARCAS program was previously used to simulate the condensation of $\text{Si}_x\text{Ge}_{1-x}$ clusters [14], where the stability of the cluster shapes was left as an unanswered question. Each condensation run was 50 ns long, but the temperature of the clusters, while momentarily reaching values close to 1700 K, dropped to 300 K within 20–30 ns. While this high temperature exceeds the natural melting points of both Si (1687 K) and Ge (1211 K), it has been shown that the Tersoff potential overestimates the melting point of Si to about 2400 K [21]. To study the effect of melting on the mobility of the cluster atoms, annealing temperatures on both sides of the potential-dictated melting points were deemed suitable. Thus, for the current work, eleven of the least spherical of the clusters were further annealed using PARCAS for consecutive runs of 100 ns at both 1800 K and 3000 K to see whether or not their sphericity would improve. Runs at the extreme temperature of 6000 K were also performed for the sake of comparison. All clusters were returned to 300 K at the end of each annealing run. The clusters contained 1031 atoms each with a variety of different Si-to-Ge concentration ratios.

The addition of the semi-grand-canonical Monte Carlo algorithm to the LAMMPS source code gives rise to a method wherein once every specified amount of MD time steps, a number of Monte Carlo swapping attempts are performed. A single attempt consists of choosing a cluster atom and testing whether swapping the atom type (here, from Si to Ge or vice versa) would reduce the energy of the system by more than a certain threshold energy $\Delta\mu$. If so, the swap is made permanent, and the velocity of the atom is rescaled to conserve its kinetic energy; if not, the swap persists only if

$$\exp\left(-\frac{\Delta E \pm \Delta\mu}{k_B T}\right) > N_{rand}, \quad (1)$$

where ΔE is the change in energy of the system after the swap, k_B the Boltzmann constant, T the temperature of the simulation and N_{rand} a computer-generated random number between 0 and 1. The sign in front of $\Delta\mu$ depends on the direction of the swap. In physical terms, μ is the element-specific chemical potential, whence $\Delta\mu$ is the difference thereof for the two elements in question, and is assigned a value by the user.

Without the application of the swap condition in Eq. (1), a simulated cluster would quickly become monoelemental due to the difference in energetics of the elements present in the cluster. While this would result in the smallest possible system energy, the respective amounts of atoms have to be conserved for the simulation to be physical. Setting a value for $\Delta\mu$ defines a probability for individual atoms of the less favorable element to remain in the cluster, and fine-tuning this probability assures that the element ratio fluctuates around its original value throughout the simulation. This results in a shortcut in which the slow process of MD diffusion can be achieved in a fraction of the CPU time. This is also faster than simply swapping neighboring atom types, since atoms can now instantly migrate to the other side of the cluster. The only problem with this approach is that the shortcut takes rather directly to thermal equilibrium, skipping any potential local minima that may exist as intermediate cluster structures, even experimental ones.

The SGCMC method was used for multiple purposes. First, a number of the more spherical clusters obtained in our previous work were further simulated for 1 ns at 300 K using the SGCMC algorithm, keeping track of the element distribution and the total energy of the system. Then, new spherical clusters of 1015 atoms with a starting configuration of 50% Ge in the core and 50% Si on the outer layers were built from scratch and simulated for 1 ns at

300 K to check for Ge segregation. These simulations included a thorough array of different values of $\Delta\mu$ to span the entire $\text{Si}_x\text{Ge}_{1-x}$ concentration spectrum.

3. Theoretical quantities

The structure of the simulated clusters is investigated primarily in terms of four quantities: sphericity, crystallinity, free energy, and Ge surface segregation. We use the same definition as in our previous work for the sphericity $S = V_c/V_{max}$, where

$$V_c = \sum_i \frac{N_i}{\rho_i} \quad (2)$$

is the total volume taken up by a cluster having N atoms of elements i with densities of ρ_i , and

$$V_{max} = \frac{4}{3}\pi r_{max}^3 \quad (3)$$

is the volume encompassed by a hypothetical spherical cluster with the same radius as the maximum atom distance r_{max} from the center of mass of the actual cluster. Thus, for a perfect sphere, $S = 1.0$, while for the least spherical clusters used in this work, S varies in the range 0.1–0.3.

The crystallinity of the clusters is analyzed using the structure parameter P_{st} , which is defined as

$$P_{st}(i) = \frac{1}{p_u(i)} \left(\sum_j (\theta_i(j) - \theta_j^p)^2 \right)^{1/2} \quad (4)$$

$$p_u(i) = \left(\sum_j (\theta_i^u(j) - \theta_j^p)^2 \right)^{1/2}$$

where $\theta_i(j)$ is a list of the $n_{nb}(n_{nb} - 1)/2$ angles formed between atom i and its n_{nb} nearest neighbors. The number n_{nb} is determined from the ideal crystal structure, and is 4 for the diamond structure (both Si and Ge). θ_j^p is the distribution of angles in a perfect lattice and $\theta_i^u(j) = j\pi/n_{nb}(n_{nb} - 1)/2$ the uniform angular distribution [24]. The structure parameter can thus be used to determine how well the atoms in a cluster settle into a lattice formation according to their relative angles; for reference, $P_{st} = 0$ for all atoms of a perfect crystal lattice, and a distribution of values below $P_{st} = 0.2$ indicates that the clusters are primarily crystalline.

The free energy of a cluster is

$$F = E - TS, \quad (5)$$

where $E = E_{kin} + E_{pot}$ corresponds to the total energy of the system, a value calculated at each simulation output step as the sum of the kinetic and potential energies of each atom. While the temperature T is always the same (300 K) at the beginning and the end of each simulation, the entropy S increases as the system, regardless of the simulation method, approaches a state of equilibrium, wherein the potential energy is also minimized. This means that simulated clusters evolve towards a structure where the free energy is as small as possible. Energy values calculated using the same potential should ideally be the same in different MD programs, but additional simulation parameters may cause a slight difference. Therefore, all runs are finalized with the PARCAS program to ascertain an equivalent basis of comparison.

Surface segregation, as a measure of the average distances of the atoms of each element from the center of mass of the cluster, is not unequivocally quantifiable, since these distances depend on the amount of atoms of each element present in the cluster. However, the effect of segregation can be studied qualitatively by simply comparing these distances, where any pronounced differences make segregation clearly visible.

Table 1

Improvement of sphericity and potential energy with annealing, averaged over all runs (44 clusters). For comparison, the values are listed for SGCMC runs of perfect spheres. The energy of these spheres is subtracted from all values, shown in eV/atom.

	Sphericity	Energy
Pre-anneal	0.2798	0.1065
1800 K	0.3243	0.0947
3000 K	0.3633	0.0791
6000 K	0.5190	0.0170
SGCMC	0.9782	0.0000

4. Results

4.1. Kinetics: MD simulations

The numerical results for the MD annealings are given in Table 1. While the sphericity increases and the potential energy decreases in nearly all individual runs, the magnitude of these effects is random in nature. Moreover, the original clusters have slightly differing sphericity and energy values to begin with, due to the finite number of available results from our previous study. Thus, it is most sensible to average the final values for all clusters when considering the amount of improvement from the pre-annealed clusters.

Surprisingly, the aforementioned melting seems to have little effect on the results of the annealing: the effects on sphericity and potential energy are only slightly more pronounced in the 3000 K annealings than in the 1800 K ones, although annealing at neither temperature results in distinct improvements from prior to annealing. Annealing at 6000 K has a more definite effect in terms of potential energy, but the sphericity does not improve much beyond 0.5 on average. In all runs, all of the increase in sphericity and decrease in potential energy happens during the first 100 ns of annealing.

The crystallinity of the annealed clusters changes very little when annealed at 1800 K or 3000 K, as is apparent in Fig. 1. While a distribution peak just below 0.2 implies a primarily crystalline angular distribution, the shape of the curve means that the clusters contain nanocrystalline regions that are not aligned with each other [14]. At these temperatures, annealing cannot improve this distribution further to make single crystals out of the clusters. However, some of the clusters annealed at 6000 K do cross the bar-

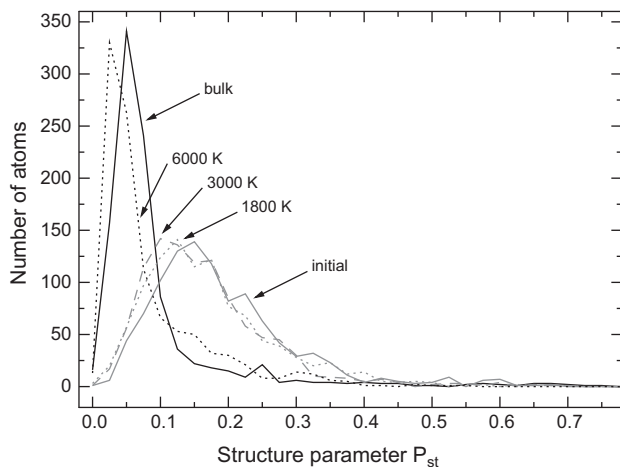


Fig. 1. Distribution of the structure parameter P_{st} in the clusters prior to annealing (grey solid line), after annealing at 1800 K (grey dotted line), after annealing at 3000 K (grey dashed line), and after annealing at 6000 K (black dotted line). For comparison, the distribution is also shown for one of the clusters cut out from crystalline bulk and simulated with the SGCMC algorithm (black solid line).

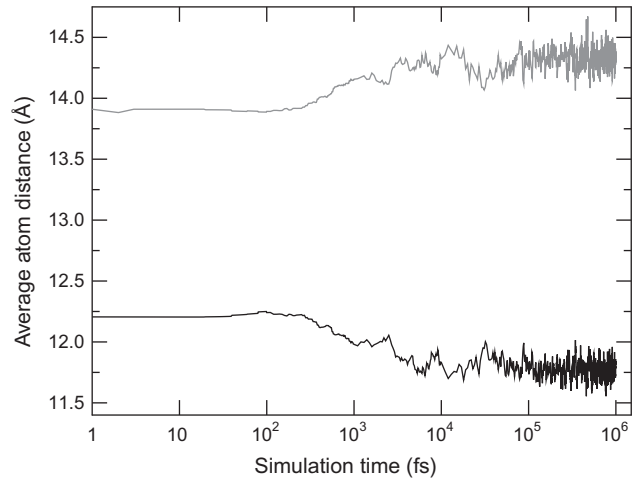


Fig. 2. Average atom distance from the center of mass of the cluster for Si (black) and Ge (grey) as a function of simulation time for a condensed cluster further simulated using the SGCMC algorithm.

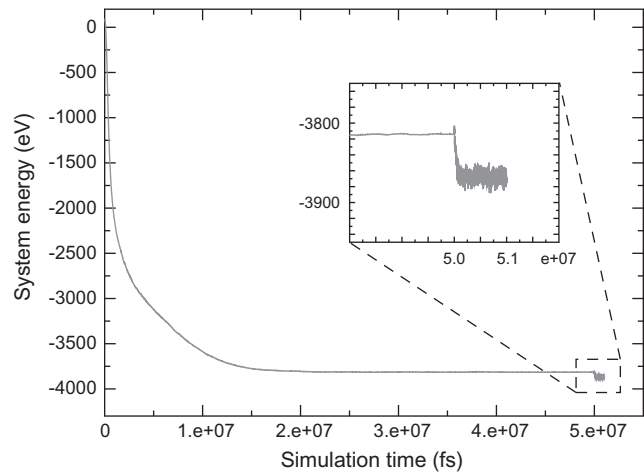


Fig. 3. System energy as a function of simulation time for a cluster condensation (up to 50 ns) and the ensuing SGCMC run (inset graph).

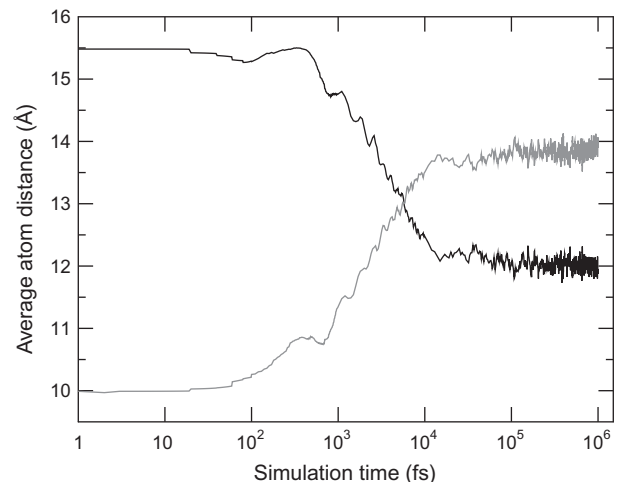


Fig. 4. Average atom distance from the center of mass of the cluster for Si (black) and Ge (grey) as a function of simulation time for a spherical cluster cut out from crystalline bulk simulated using the SGCMC algorithm, starting with all Ge atoms inside and all Si atoms on the outer shells.

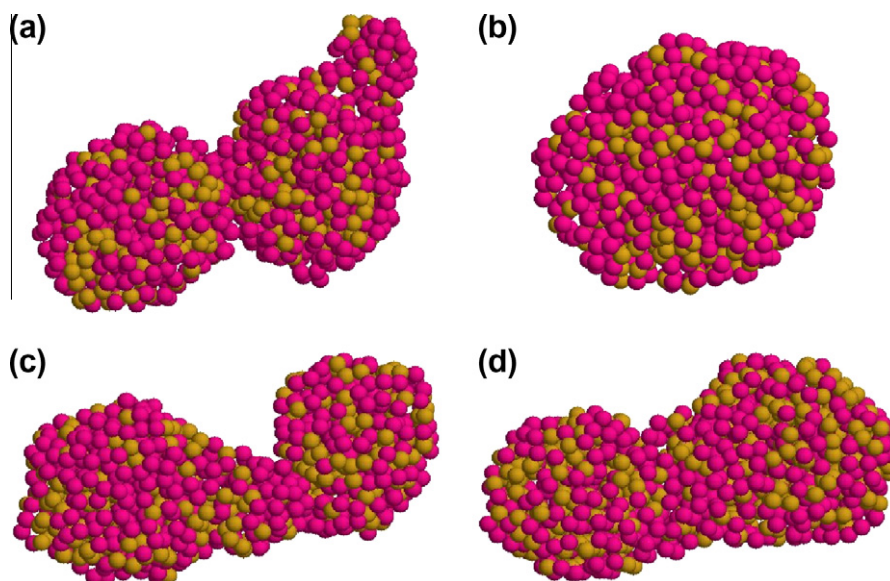


Fig. 5. Visual representation of the effect of annealing. On the top row, a cluster (a) prior to and (b) after annealing at 6000 K, where sphericity improves from 0.16 to 0.60. On the bottom row, a cluster (c) prior to and (d) after annealing at 6000 K, where sphericity improves from 0.18 to 0.41.

rier and become as crystalline as the cut-out clusters, which is also apparent when studying the energy level shown in Table 1.

Any further Ge surface segregation caused by the annealing simulations alone cannot adequately be studied, since the sphericity of the clusters changes drastically, which decreases the average atom distances for both elements.

4.2. Thermodynamics: SGCMC simulations

Simulating some of the previously condensed clusters using the SGCMC algorithm reveals that the surface segregation of Ge atoms is energetically favorable, as can be seen from Figs. 2 and 3. This result is further confirmed by simulating a perfect crystalline $\text{Si}_{0.5}\text{Ge}_{0.5}$ sphere with all Ge atoms originally in the center. The distance graph of Fig. 4 shows that the Ge atoms quickly migrate towards the surface of the sphere.

The comprehensive results from the sphere simulations are used to determine a relationship between chemical potential, Ge atom percentage, and potential energy. The first quantity is a user-defined parameter of no interest in this study; only the last two represent results of any significance. Since a relaxed crystalline structure with Ge on the outer layers represents the ideal cluster in terms of potential energy, this state is used as a reference point for the results from the other simulations shown in Table 1.

5. Discussion and conclusions

The reluctance of all annealed clusters to improve their sphericity beyond a certain limit indicates that the clusters may settle into deep local energy minima in configurations that are far from our definition of spherical. These “offending” shapes are spheres elongated in one direction, reminiscent of capsules or beans, that do not reach a high level of sphericity in spite of having considerably decreased their surface-to-volume ratio from the pre-annealing shape. This effect is illustrated in Fig. 5.

The consistent decrease of the potential energy of the clusters suggests that the annealings were at least partly successful. A comparison of the energies of the clusters annealed at the lower temperatures and the energies of the new spherical clusters cut out from bulk and simulated with SGCMC shows that the latter settle

at a considerably lower energy level. This is primarily due to the fact that these clusters were perfectly crystalline from the start. This is confirmed by the fact that those clusters annealed at 6000 K that became more crystalline also reached a low energy level comparable to that of the SGCMC clusters. There is a clear gap in Table 1 of about 0.06 eV/atom between the energy levels of the crystalline and amorphous clusters; because sphericity improved much less than potential energy in the 6000 K annealings, this gap can be attributed mostly to differences in crystallinity, while the remaining energy difference as compared to the SGCMC clusters is due to an increased sphericity.

The annealing temperature of 6000 K is close to the upper limit at which these simulations can be performed. Already the results of some runs had to be discarded because the clusters evaporated completely at the beginning of the run. Thus, it is clear that it is not possible to reach the perfect cluster shape using MD annealing. While the elongated, crystalline spheres are quite close to perfect, the minute differences in atomic position required for better sphericity cannot be surmounted in these simulations.

In conjunction with our previous work, the results presented here show that MD simulations of bottom-up methods of cluster formation result in clusters that cannot be characterized as ideal. Numerous experimental results have shown that cluster sources produce crystalline spheres of silicon (e.g. [25]), and we can indeed confirm that a near-perfect sphere is the most energetically favorable shape; nevertheless, it is impossible to determine the exact sphericity of experimental clusters, which may actually be considerably lower than 1.0. Bridging the gap between simulations of freshly condensed samples and their ideal counterparts could be accomplished with genetic algorithm simulations, but this would give no insight into whether real clusters can reach their ideal shapes through diffusion in macroscopic time scales. We can only surmise that an annealing temperature of 6000 K, while physically questionable and far from the original scope of the potential used, represents an increase in the rate of diffusion that allows for comparison between simulations and the real world.

Acknowledgement

Prof. Karsten Albe is gratefully acknowledged for the useful discussion during the drafting of this article.

References

- [1] P. Jensen, P. Mélinon, M. Treilleux, A. Hoareau, J.X. Hu, G. Fuchs, B. Cabaud, Nucl. Instr. Meth. B 79 (1993) 219.
- [2] P. Mélinon, V. Paillard, V. Dupuis, A. Perez, P. Jensen, A. Hoareau, J.P. Perez, J. Tuaille, M. Broyer, J.L. Vialle, M. Pellarin, B. Baguenard, J. Lermé, Int. J. Mod. Phys. B 9 (1995) 339.
- [3] C. Binns, Surf. Sci. Rep. 44 (2001) 1.
- [4] A. Perez, P. Mélinon, V. Paillard, V. Dupuis, P. Jensen, A. Hoareau, J.P. Perez, J. Tuaille, M. Broyer, J.L. Vialle, M. Pellarin, B. Baguenard, J. Lermé, Nanostruct. Mater. 6 (1995) 43.
- [5] A. Perez, P. Mélinon, V. Dupuis, P. Jensen, B. Prével, J. Tuaille, L. Bardotti, C. Martet, M. Treilleux, M. Broyer, M. Pellarin, J.L. Vaille, B. Palpant, J. Lermé, J. Phys. D 30 (1997) 709.
- [6] P. Mélinon, P. Kéghélian, B. Prével, A. Perez, G. Guiraud, J. LeBrusq, J. Lermé, M. Pellarin, M. Broyer, J. Chem. Phys. 107 (1997) 10278.
- [7] V. Lehmann, U. Gösele, Appl. Phys. Lett. 58 (1991) 856.
- [8] L.T. Canham, Appl. Phys. Lett. 57 (1990) 1046.
- [9] R. Venkatasubramanian et al., Appl. Phys. Lett. 59 (13) (1991) 1603.
- [10] S. Gardelis et al., Appl. Phys. Lett. 59 (17) (1991) 2118.
- [11] H. Haberland, Z. Insepov, M. Moseler, Phys. Rev. B 51 (1995) 11061.
- [12] A. Harjunmaa, J. Tarus, K. Nordlund, J. Keinonen, Eur. Phys. J. D 43 (2007) 165.
- [13] K. Meinander, Growth and Modification of Cluster-assembled Thin Films, PhD Thesis, University of Helsinki, 2009.
- [14] A. Harjunmaa, K. Nordlund, Comp. Mater. Sci. 47 (2009) 456.
- [15] J. Tarus, M. Tantarimäki, K. Nordlund, Nucl. Instr. Meth. B 228 (2005) 51.
- [16] B.J. Alder, T.E. Wainwright, J. Chem. Phys. 27 (1957) 1208.
- [17] K. Nordlund, *PARCAS* Computer Code. The Main Principles of the Molecular Dynamics Algorithms are Presented in [21,22]. The Adaptive Time Step and Electronic Stopping Algorithms are the Same as in [23].
- [18] S. Plimpton, J. Comp. Phys. 117 (1995) 1. <<http://lammps.sandia.gov/>>.
- [19] J. Tersoff, Phys. Rev. B 39 (1989) 5566.
- [20] H.J.C. Berendsen, J.P.M. Postma, W.F. van Gunsteren, A. DiNola, J.R. Haak, J. Chem. Phys. 81 (1984) 3684.
- [21] K. Nordlund, M. Ghaly, R.S. Averback, M. Caturla, T. Diaz de la Rubia, J. Tarus, Phys. Rev. B 57 (1998) 7556.
- [22] M. Ghaly, K. Nordlund, R.S. Averback, Philos. Mag. A 79 (1999) 795.
- [23] K. Nordlund, Comp. Mater. Sci. 3 (1995) 448.
- [24] K. Nordlund, R.S. Averback, Phys. Rev. B 56 (1997) 2421.
- [25] M.A. Laguna, V. Paillard, B. Kohn, M. Ehbrecht, F. Huisken, G. Ledoux, R. Papoular, H. Hofmeister, J. Lumin. 80 (1998) 223.